

# Estimation of Non-uniform Sediment Discharge Using Actual Results of Dam Reservoir Sedimentation

**Tomoyuki Suzuki**

*Assistant Manager, Dr. Eng., Engineering Dept.,  
Planning Division, INA Corporation, Japan*

**Josuke Kashiwai**

*Team Leader, River and Dam Hydraulic Engineering Team,  
Hydraulic Engineering Research Group,  
Public Works Research Institute, Japan*

**Yoshihiro Yoshioka**

*Kashiwazaki Regional Office, Niigata Prefecture, Japan*

## 1. Introduction

The dams with the sedimentation volume exceeding or approaching their design storage capacity start to appear due to the greater-than-designed sediment inflow and the increasing of management years. It is an urgent matter to investigate and implement measures to combat sedimentation in these dams. In order to devise the most appropriate measures for each dam, however, it is necessary to have an accurate picture of sedimentation conditions and to formulate dependable forecasts of future sedimentation likely to result from any adopted measures. A numerical model for the riverbed variation is a useful tool for such forecasts, but requires accurate estimates of sediment inflow: a key boundary condition of the model.

One set of parameters necessary for such a simulation is the relationship between the flow rate and the sediment discharge for each typical within a dam deposit. The relationship can be obtained by combining data from monitoring records at each dam with the results of additional surveys, however, the estimating procedures have not to be established yet.

We recently obtained the opportunity to estimate the sediment discharge at the Sabaishigawa Dam, Niigata Prefecture, which is one of the dams facing the urgent sedimentation problems. Additional surveys included boring of dam deposit and sampling of inflow and outflow water during flood, and we gathered the detailed information of sediment diameter in the river and analyzed using the hydrologic data and the annual sedimentation records. As a result, we obtained the relationship between the flow rate and the sediment discharge reproducing fairly well the annual sedimentation records. This paper describes the estimation method for sediment discharge and its validity.

While this study investigates conditions solely at the Sabaishigawa Dam, we attempted to systematize the survey methods and analytical procedures to provide a framework for similar investigations at other sites. In the dam, a large amount of fine sediment

passes through the reservoir. We developed a procedure for estimating a trap ratio of the sediment inflow (trap efficiency) from numerical simulations. The contents appear to be of general utility in studies of this type.

## 2. Overview of Estimation Method

### 2.1 Flowchart of general procedure

The flowchart in Fig. 1 shows the procedure we propose. The method is based on the actual records for dam sedimentation. A relationship between the flow rate and the sediment discharge can be identified for each typical particle size contained in dam deposit.

### 2.2 Classifying dam deposit by sediment tarp condition

We use surveyed data for boring, sedimentation topography, etc. to determine the spatial distribution of sediment diameter within a dam deposit. The deposit can be classified as either "completely trapped sediment", which is completely trapped within a reservoir because of coarse particle, or "partially trapped sediment" that is partially trapped in a reservoir because of fine particle (①: means "1st step"). The threshold diameter that distinguishes these two types is unique for each reservoir, and is different from the conventional classification of bed load, suspended load and wash load. Here, we assume that the bed load is not included in the partially trapped.

### 2.3 Estimation of sediment discharge for the completely trapped particles

First, the upstream riverbed is analyzed to find the typical cross section and gradient, and we examine how accurately the bed load and suspended load are predicted by the formulas generally used by researchers (②). For this assessment, the minimum discharge in which sediment transport occurs (critical discharge  $Q_c$ ) is also considered as a parameter. The index of applicability of the formula is the annual sedi-

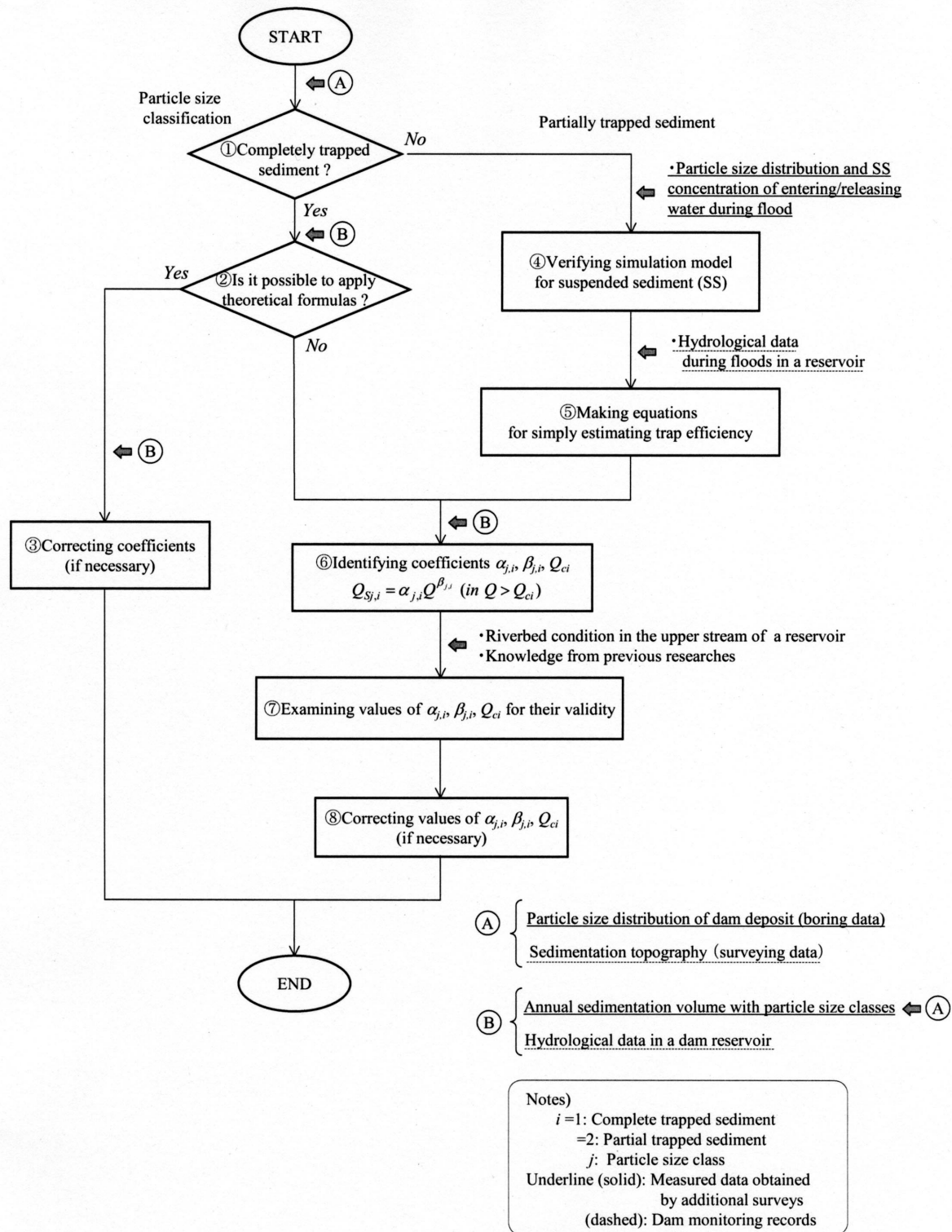


Fig. 1 Flowchart of procedure for estimating "non-uniform" sediment discharge

mentation volumes with the typical particle sizes, which can be calculated using the spatial distribution of sediment diameter from the boring survey and the annual sedimentation volume. If the formula is considered to be valid, it is then used to estimate the sediment discharge of the completely trapped sediment.

When there is much bare rock and armoring upstream of a reservoir, or when the completely trapped sediment contains a large amount of fine sedi-

ment, the sediment influx volume given by the formula commonly diverges significantly from the actual sedimentation volume. In such cases, the formula is considered to be meaningless. This situation is encountered in our study at Sabaishigawa Dam. The simple exponential function shown below is used to relate the sediment flow rate  $Q_{Sj}$  of the typical particle class ( $j$ ) to the river flow rate  $Q$ . The variables  $\alpha$ ,  $\beta$  and  $Q_c$  are identified from the actual deposit volumes (the annual

sedimentation volume for each typical particle size; (6).

$$Q_{Sj} = \alpha_j Q^{\beta_j} \quad (Q > Q_c) \quad (1)$$

The above equation is usually used to describe the relationship between the wash load and the flow rate. An equation of the same form is used later for the partially trapped sediment. The obtained values of coefficients and critical discharge are verified and corrected if necessary (7, 8).

#### 2.4 Estimation of sediment discharge for the partially trapped particles

Equation (1) is used to find the coefficients and critical discharges for inflow of the partially trapped sediment, just as for the completely trapped one when the formula is inapplicable. However, as some of the inflow of fine sediment usually passes through a reservoir, the passing volume must be subtracted from the inflow volume calculated using Eq.(1) to obtain the trapped volume. The following equation is used to calculate the trap efficiency  $\gamma_{jk}$  for the typical particle class ( $j$ ) under flood ( $k$ ), yielding the annual sedimentation volume  $[V_{Sj}]_i$  during year ( $i$ ).

$$[V_{Sj}]_i = \sum_{k=1}^{n_i} \gamma_{jk} \int_k Q_{Sj} dt = \sum_{k=1}^{n_i} \gamma_{jk} \int_k \alpha_j Q^{\beta_j} dt \quad (2)$$

Here,  $n_i$  represents the number of floods above the critical discharge during year ( $i$ ).

The trap efficiency  $\gamma_{jk}$  is estimated using a numerical simulation model whose validity has been demonstrated from observed data from the water sampling during floods (4,5). A simple method for estimating  $\gamma_{jk}$ , which is explained in detail in Chapter 3.5, is desired as it would have required much time and labor to carry out simulations of "all past floods".

In the following section, we show how the above procedure is used to determine sediment discharge at the Sabaishigawa Dam.

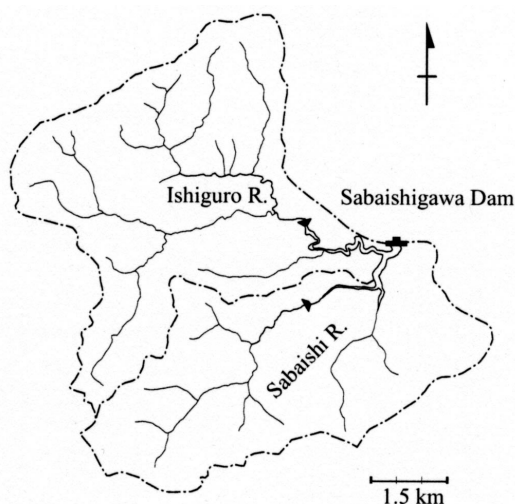


Fig. 2 Sabaishigawa dam and its catchment basin

### 3. Estimation of Sediment Discharge at Sabaishigawa Dam

#### 3.1 Overview of Sabaishigawa Dam

Figure 2 shows a catchment area of the Sabaishigawa Dam. The dam is on the Sabaishi River, the class B river running through the city of Kashiwazaki, Niigata Prefecture. The gravity-type concrete dam is 37 m high and 170 m wide and has a reservoir capacity of 6,000,000 m<sup>3</sup>. The dam is multipurpose, with the chief purposes of flood control and supply of irrigation water. Construction was completed in 1974. The dam is also fed by the Ishiguro River, and the two rivers account for 85% of the 46 km<sup>2</sup> catchment area of the dam. The reservoir is made up mainly of the former valleys of the Sabaishi and Ishiguro Rivers and comprises the junction of the rivers.

Much of the sediment discharge to the dam enters within flood waters following rains in the summer, autumn seasons, and during runoff associated with spring thaw. The flood history detailed in Fig. 3 shows that floods with peak discharges in excess of 100 m<sup>3</sup>/s occurred 5 times in the 29 years since the dam was constructed. Discharges exceeding 40 m<sup>3</sup>/s occurred approximately yearly during that period. Discharge during spring run-off varied greatly from year to year, but was in the range of 20 – 30 m<sup>3</sup>/s for periods of about 60 days in the years of greatest runoff. The reservoir water level is usually lowered during periods of the spring run-off, and this operation would have released the accumulated sediment downstream of the dam.

Figures 4 show variations in the longitudinal topography of sedimentation over past years. Fig. 4(a) shows the section from the junction to the Ishiguro valley upstream, while Fig. 4(b) shows the section from the dam to the Sabaishi valley upstream. Sedimentation occurred throughout the reservoir, and no significant differences in sedimentation form were observed between the Sabaishi and the Ishiguro valleys. Sedimentation delta wasn't clearly observed in both valleys. This was probably due to the accumulation of large amount of fine sediment and the effects of lowering the reservoir water level.

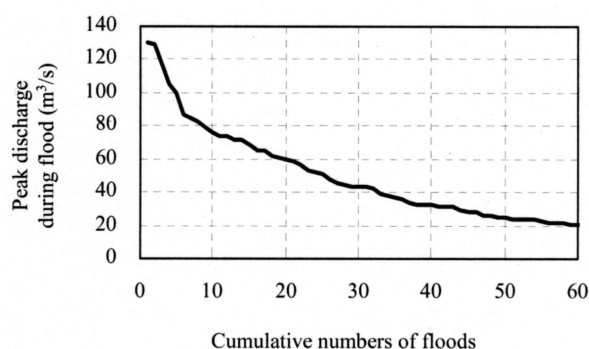
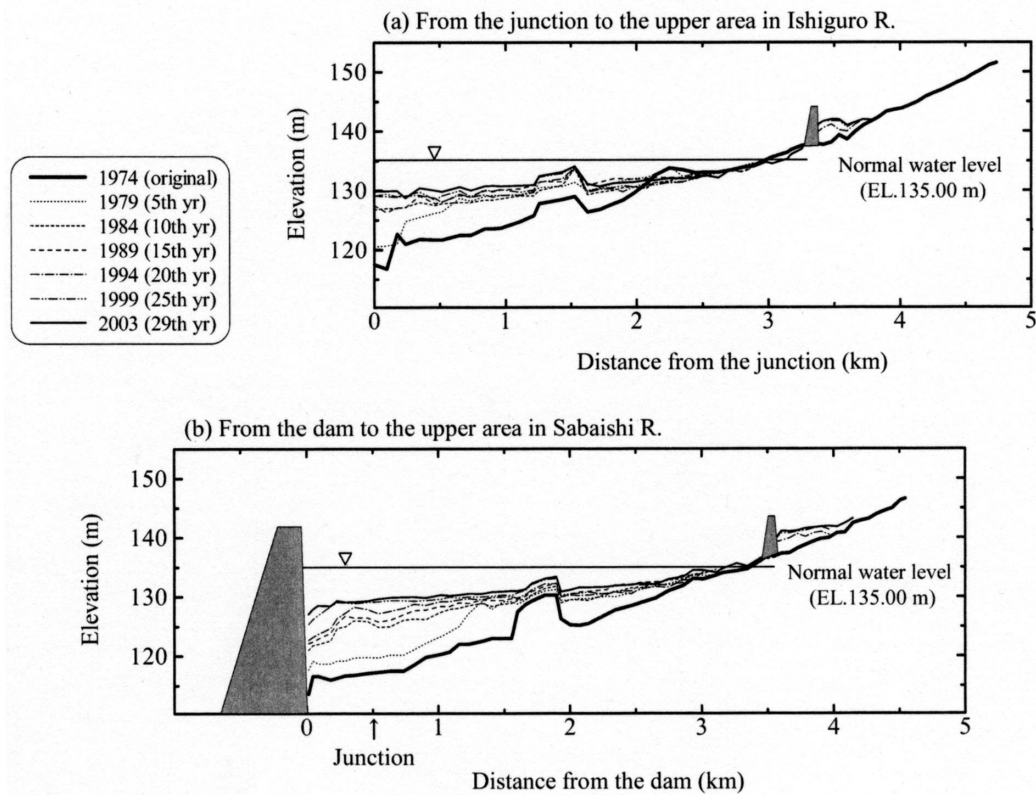


Fig. 3 Cumulative numbers of floods (1974-2002) (excepting floods of melted snow)



Figs. 4 Temporal changes in longitudinal topography

Table 1 List of data used in this study

Survey Item	Data Item	Chief Objective	Specifications (in case of Sabaishigawa Dam)
Dam monitoring records	Water discharge	Estimating trap efficiency; Selecting sedimentation record; Numerical simulation	At 10 min–1 hr intervals (peak flood > 30 m <sup>3</sup> /s)
		Estimating trap efficiency; Selecting sedimentation record	Daily mean (over season)
	Water level	Selecting sedimentation record	Daily mean (over season)
		Numerical simulation	At 10 min–1 hr intervals (flood only)
Topographic survey of dam deposit	Longitudinal shape	Setting locations for boring	Every year (entire period)
	Cross sectional shape	Calculating sedimentation volume; Numerical simulation	
Boring of dam deposit	Particle size distribution	Classifying dam deposit by particle size; Calculating annual sedimentation volume with typical particle size classes	Vertical profiles (1 m increments) at 18 locations (conducted in 2002)
	Porosity		
Water sampling during flood	SS concentration	Examining characteristics of SS discharge; Verifying simulation model; Verifying estimated values of coefficients $\alpha$ , $\beta$	10 – 12 samples each taken at up/down-stream of a reservoir (conducted in 2003)
	SS size distribution		

### 3.2 Data used in this study

Table 1 shows the data used for this study. In the table, the dam monitoring records and the sedimentation topographic data are regularly accumulated by the dam management office in Japan. The boring of dam deposit and the water sampling are additional surveys for the study, which have been carried out in 2002, 2003. Figure 5 shows the locations of the additional surveys.

### 3.3 Particle size classification of dam deposit

Fig. 6 presents the particle size distributions of dam deposit calculated from the boring results and the sedimentation volume records. The figure indicates that all of the three zones had nearly identical patterns of distribution; particles less than 100  $\mu\text{m}$  in size accounted for about 80% of the entire sedimentation volume. The measured relationship between  $D_{60}$  and porosity is typical for dams in Japan<sup>2)</sup>.

Fig. 7 shows the particle size distribution of sedi-

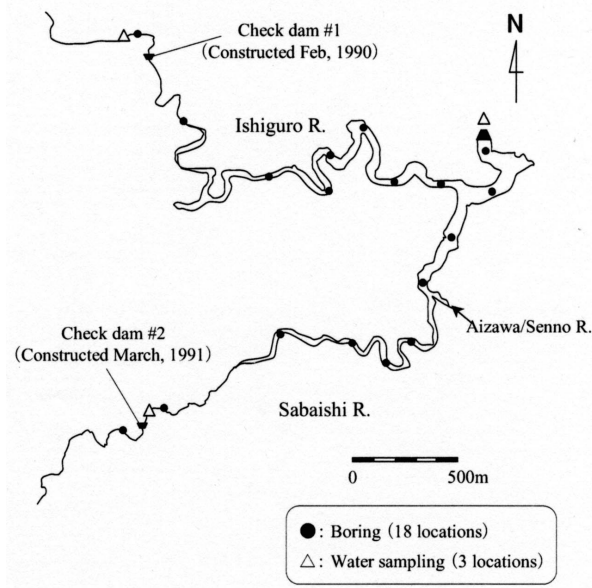


Fig. 5 Locations of additional surveys

ment deposited just upstream of the dam. The sediment  $> 250 \mu\text{m}$  in size was hardly contained. This information indicates that the sediment  $> 250 \mu\text{m}$  were almost completely trapped upstream of the dam.

Fig. 8 shows longitudinal variations of particle size distribution in the dam, within the Sabaishi Valley. Some sediment coarser than  $250 \mu\text{m}$  was found in the vicinity of the river junction, but this sediment did not extend to the dam. Upstream of the junction, the observed sediments varied gradationally between coarse and fine, and Fig. 8 is probably a good representation of the sediment constituents. From the above observations,  $250 \mu\text{m}$  was selected as the diameter that represents the boundary between complete and partial trapping. As a result, the partially trapped sediment makes up about 90% of the total sedimentation volume at the dam, a very high fraction. It is therefore more important to predict the estimation of the partially trapped sediment than of the completely trapped at this dam. As shown in Table 2, when this diameter is used, we classified six particle diameter classes finer than  $250 \mu\text{m}$  and four classes larger than  $250 \mu\text{m}$ , and attempted to estimate discharge of these 10 size classes.

Coarse sediment was contained near the 1 and 2 km upstream from the dam much more than other area (Fig. 8). While no clear explanation has been found for this, it is likely that a contributing cause at the 1 km site is the presence of a tributary (Aizawa/Senno Riv.) just upstream from that location (see Fig. 5), which would be expected to increase the mean flow speed and reduce the accumulation of the fine sediment. Other possible factors are the change of the reservoir cross sectional shape in the longitudinal direction, but no relationship was observed between this factor and the phenomenon.

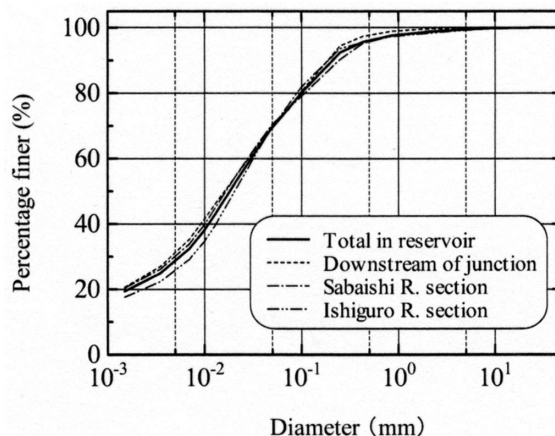


Fig. 6 Particle size distributions of the dam deposit ("Downstream of junction" in the legend means the zone between the dam and the junction of the rivers, "Sabaishi R. section" means the Sabaishi valley upstream of the junction, and "Ishiguro R. section" means the Ishiguro valley upstream of the junction.)

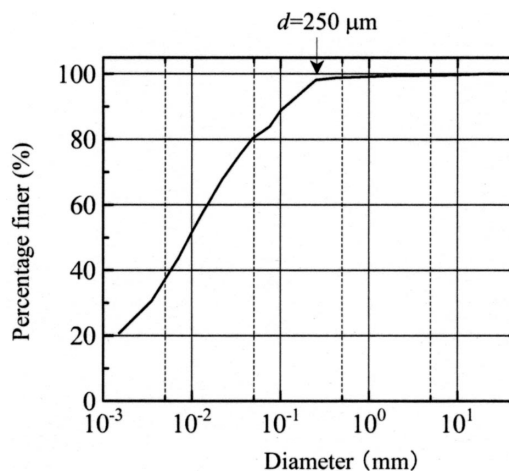


Fig. 7 Particle size distributions of the dam deposit (just upstream of the dam)

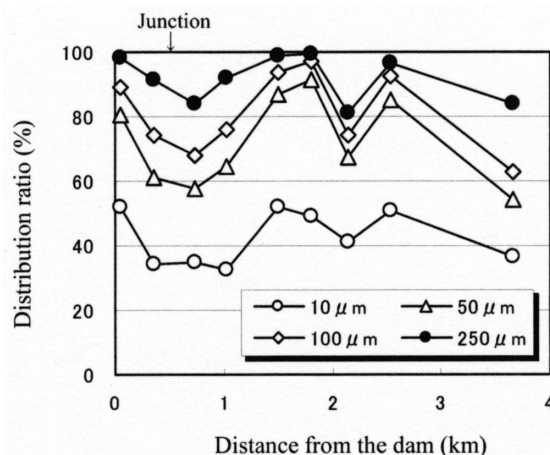


Fig. 8 Longitudinal variations of particle size distribution ratio of the dam deposit (example: Sabaishi R. section)

Table 2 Particle size classification

	Class #	Size range (mm)	Typical size (mm)
Partially trapped	1	- 0.0035	0.0035
	2	0.0035 - 0.010	0.0059
	3	0.010 - 0.022	0.015
	4	0.022 - 0.048	0.032
	5	0.048 - 0.10	0.069
	6	0.10 - 0.25	0.16
Completely trapped	7	0.25 - 0.85	0.46
	8	0.85 - 4.8	2.0
	9	4.8 - 19	9.5
	10	19 - 38	27

### 3.4 Estimation of sediment discharge for the completely trapped particles

We initially attempted the estimation using the Ashida and Michiue's formulas for sediment discharge (bed load, Ref. 3; suspended load, Ref. 4), but the prediction far exceeded the observed. This indicates that the sediment supply is far less than the carrying capacity of the river channel. We therefore concluded that the formulas were not applicable to this river channel. The coefficients  $\alpha$ ,  $\beta$  and  $Q_c$  were therefore determined from Eq.(1) "the simple exponential expression". For the completely trapped sediment,  $\beta$  and  $Q_c$  were selected to minimize the residue of the following:

$$\tilde{\epsilon}_j = \sum_{i=1}^N \left| [\tilde{V}_{S0j}]_i - [\tilde{V}_{Sj}]_i \right| \quad (3)$$

Here,  $N$  is the number of years in the period of interest, and  $[V_{S0j}]_i$  and  $[V_{Sj}]_i$  are the measured and estimated dimensionless annual volumes of sediments of size class ( $j$ ) during the period, respectively. The values are given by the following equations:

$$[\tilde{V}_{S0j}]_i = [V_{S0j}]_i / \sum_{m=1}^N [V_{S0j}]_m \quad (4)$$

$$\begin{aligned} [\tilde{V}_{Sj}]_i &= [V_{Sj}]_i / \sum_{m=1}^N [V_{Sj}]_m \\ &= \sum_{k=1}^{n_j} \gamma_{jk} \int_k Q^{\beta_j} dt / \sum_{m=1}^N \sum_{k=1}^{n_m} \gamma_{jk} \int_k Q^{\beta_j} dt \end{aligned} \quad (5)$$

Here,  $[V_{S0j}]_i$  in Eq.(4) is the measured volume of sediments of size class ( $j$ ) during year ( $i$ ), and the trap efficiency  $\gamma$  in Eq.(5) is 1 for the completely trapped sediment.  $[V_{Sj}]_i$  in Eq.(5) is substituted into Eq.(2).  $\alpha$  is also eliminated by the process that eliminates the dimensions. Therefore,  $\beta$  and  $Q_c$  are identified in Eq.(3). As reference in the search for values for  $\beta$ , the previous observations have been reported  $\beta = 2 \sim 3$ ; the value of  $\beta$  was searched from 1 to 5 to cover an actual value sufficiently.  $Q_c$  values were trialed within the range between 0 and 20 m<sup>3</sup>/s. The search ranges for  $\beta$  and  $Q_c$  were set for convenience here, but in future studies, more observed data must be gathered to enable identification of these parameters by more rigorous methods.

The next task is to find  $\alpha$ . This is difficult because  $\alpha$  is considered to vary greatly with river characteristics and with particle diameter, and it is also difficult to obtain measured data. Therefore, the established values of  $\beta$  and  $Q_c$  were used in the following equation to match the estimated and measured total sedimentation volumes, and the value of  $\alpha$  was calculated backwards.

$$\alpha_j = \sum_{i=1}^N [V_{S0j}]_i / \sum_{m=1}^N \sum_{k=1}^{n_m} \gamma_{jk} \int_k Q^{\beta_j} dt \quad (6)$$

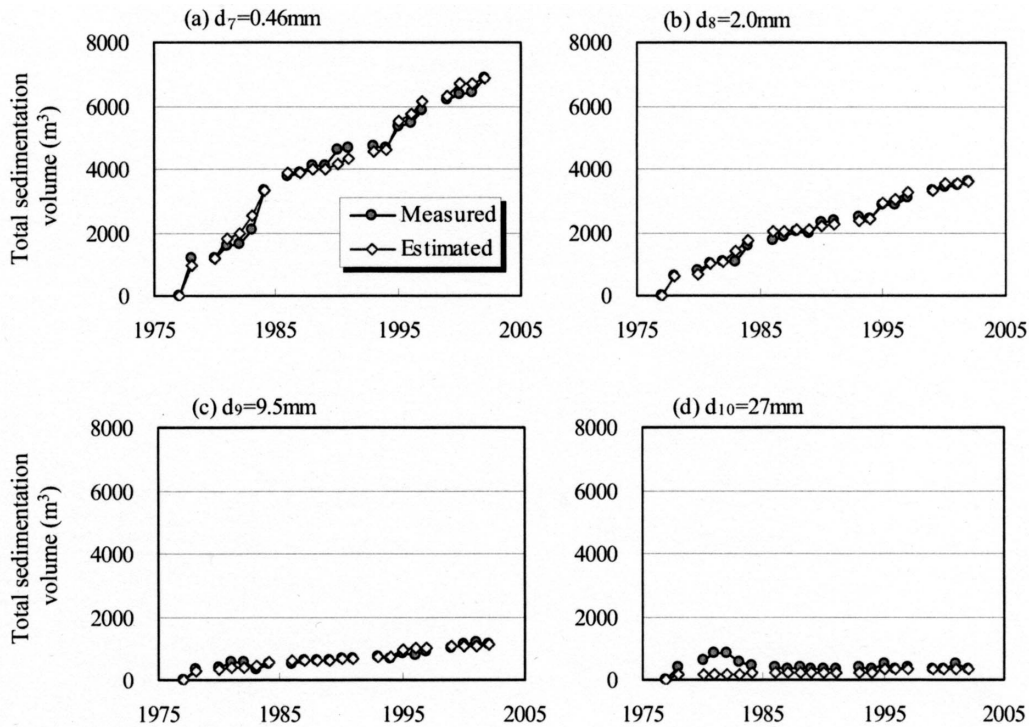
The measured data used for this exercise was the annual volume by size class  $[V_{S0j}]_i$  in Eq.(4), but there were some years in which rather large sediment volumes occurred in spite of the absence of flooding, or other unusual events occurred that obscuring any correlation between  $[V_{S0j}]_i$  and discharge. The reasons for this are unclear, but the accuracy of surveyed data for sedimentation is questionable because the number of boring and measuring points was not enough for the scale of the reservoir. Therefore, a five-term power series  $Q^m$  ( $m = 1 \sim 5$ ) was constructed and integrated for comparison with the annual sedimentation record and  $Q^m$ . Years for which almost no correlation was shown with any value of  $m$  were not used for identifying values of the variables. As a result of the data selection, we chose the measured data from 21 of the 29 years for which data was collected. The neglected sedimentation volume is not large; it represents only a small fraction of the total amount.

The annual sedimentation volumes originating from the Sabaishi and Ishiguro Rivers were distinguished as follows. Above the junction, they were distinguished by their geographic locations within either the Sabaishi valley or the Ishiguro valley. Downstream of the junction, the contributions from the two rivers were distinguished by the ratio of sediment volume at each particle class for each valley.

Table 3 shows the identified parameters, and Fig. 9 shows the estimated results for the typical particle classes in the Ishiguro River. The figures compare annual changes in accumulated sediment volumes. The blanks in the graph represent years for which data were not chosen, as described above. The calculations were good approximations of the measurements for the  $d_7$  (0.46 mm),  $d_8$  (2.0 mm), and  $d_9$  (9.5 mm) classes. There was a period during which the measured accumulated volumes of  $d_{10}$  (27 mm) were decreased. This

Table 3 Identified values of  $\alpha$ ,  $\beta$  for the completely trapped sediment

Class #	Typical (mm)	Sabaishi R.		Ishiguro R.	
		$\alpha$	$\beta$	$\alpha$	$\beta$
7	0.46	$4.9 \times 10^{-4}$	1.0	$3.1 \times 10^{-6}$	2.0
8	2.0	$1.1 \times 10^{-4}$	1.0	$8.5 \times 10^{-7}$	2.2
9	9.5	$3.1 \times 10^{-6}$	1.6	$1.7 \times 10^{-8}$	3.0
10	27	$9.0 \times 10^{-12}$	5.0	$2.8 \times 10^{-12}$	5.0
Critical discharg		$Q_c = 12 \text{ m}^3/\text{s}$		$Q_c = 12 \text{ m}^3/\text{s}$	



Figs. 9 Estimated results for the completely trapped sediment (example: Ishiguro R.)

could not be expressed, but since this class makes up a very small portion (0.1%) of the total volume, this discrepancy was considered negligible.

### 3.5 Estimation of sediment discharge for the partially trapped particles

#### 3.5.1 Verification of numerical simulation model

The partially trapped sediment was also estimated using Eq.(1). But the trap efficiency  $\gamma$  had to be estimated before the parameter identification.

A numerical model was made to estimate  $\gamma$ . The basic equations and main parameters are shown in Table 4. The model is a 1-D unsteady flow model with SS transport equations for typical size classes. Settling velocity of sediment was calculated using the Rubey's equation, and we assumed that resuspension of settled SS did not occur. The calculations were carried out using the MacCormack scheme.

We attempted to reproduce the September 2003 flood in order to demonstrate the validity of the model. In this simulation, a time series of SS concentration is required as a boundary condition at the upstream end. Here, the boundary data was given using Eq. (1), whose coefficients were determined from the data observed during the same flood. Table 5 shows the values for  $\alpha$  and  $\beta$  obtained from the observed data mentioned above, and Fig. 10 shows the relationship between the flow rate and the sediment discharge in the Sabaishi River for each size class given in Table 5. The number of the classifications was limited to 4 in order to make easier to see the trend. The suspended load for all of the classifications showed a relatively good correlation with the flow rate.

Figures 11 compare the calculation results with the observational data. These calculations were carried out by inserting  $\alpha$  and  $\beta$  for each typical diameter given in

Table 4 Basic equations and parameters for simulation model

	Basic Equation	Parameter
Continuity equation	$\frac{\partial A}{\partial t} + \frac{\partial Q}{\partial x} = 0$	$\Delta x=30(\text{m})$
Equation of flow motion	$\frac{\partial Q}{\partial t} + \frac{\partial}{\partial x} \left( \frac{Q^2}{A} \right) = -gA \left( \frac{\partial H}{\partial x} + \frac{n^2  Q  Q}{R^{4/3} A^2} \right)$	$\Delta t=0.1(\text{s})$ $n=0.03$
Equation of SS transport (each size)	$\frac{\partial (\bar{C}_j A)}{\partial t} + \frac{\partial (\bar{C}_j Q)}{\partial x} = B_{su} w_{sj} \bar{C}_j$	$B_{su}=A/h$

Note)  $A$ : Flow cross section;  $Q$ : Discharge;  $H$ : Water level;  $R$ : Hydraulic radius;  $\bar{C}_j$ : SS concentration of size class ( $j$ ) averaged in  $A$ ;  $h$ : water depth;  $n$ : Manning roughness coefficient

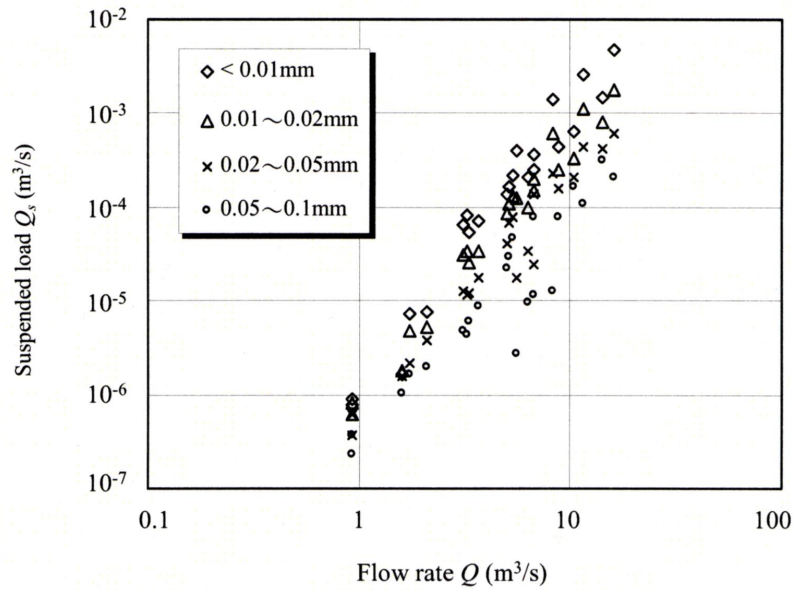


Fig. 10 Relationship between flow rate and suspended load for each particle classes (example: Sabaishi R.)

Table 5 Values of  $\alpha$ ,  $\beta$  obtained from the observed data

Size range (mm)	Sabaishi R.		Ishiguro R.	
	$\alpha$	$\beta$	$\alpha$	$\beta$
- 0.01	$1.2 \times 10^{-6}$	3.0	$4.6 \times 10^{-7}$	3.3
0.01 - 0.022	$9.2 \times 10^{-7}$	2.8	$4.8 \times 10^{-7}$	3.0
0.022 - 0.048	$5.7 \times 10^{-7}$	2.6	$3.7 \times 10^{-7}$	2.9
0.048 - 0.10	$3.4 \times 10^{-7}$	2.3	$2.9 \times 10^{-7}$	2.7

Table 2. Fig. 11(b) confirms that SS (circle mark) released from the dam is generally well reproduced by the model (see thick solid line on Fig. 11(b)). The predicted changes in the concentrations of the size classes in Fig. 11(c) also show relatively good consistency with the observed values, except for the periods of low SS concentration. Release of all the particles  $d_1 - d_4$  from the dam was observed and predicted.

The model used here is comparatively simple, but the results described above indicate that the model provides an effective approximation of the trap efficiency at the Sabaishigawa Dam.

The observations presented in Fig. 11(c) indicate that the relatively coarse component ( $d_4$ ) continued to be released after flooding. A factor that may have influenced this is the gate operation at the Sabaishigawa Dam. The dam's outlet facilities include a crest gate (elevation 135.00 m) and a hollow jet valve (normal outlet conduit, portal elevation 129.75 m). As is clear from the longitudinal topography shown in Fig. 4, the sediment just above the dam reaches almost to the level of the intake of the normal outlet conduit. The releasing water carries a large fraction of relatively coarse sediment, which settles near the surface of the sedimentation. It is likely that during the latter period of flooding, this would make up the dominant portion of the suspended load exiting the conduit, and this would explain the appearance of such high volumes at that time.

### 3.5.2 Dominant factors in trap efficiency

Although the numerical model described above is comparatively simple, it still requires much time and labor to be used for simulating historical floods. Therefore, in the alternative procedure used in this study, dominant parameters of  $\gamma$  were considered reservoir shape, flood condition,  $\alpha$  and  $\beta$ . SS simulations were made while these parameters were set at several values in order to obtain a simple expression for estimating  $\gamma$  for each typical particle class (Table 2).

Before beginning detailed descriptions of this procedure, let us first outline the relationship between  $\gamma$  and the parameters  $\alpha$ ,  $\beta$ .

Let us consider the trap efficiency  $\gamma_k$  for particles of size class ( $j$ ) during flood ( $k$ ). First, the volume of SS entering the reservoir per unit time  $Q_{sj}$  is expressed by Eq.(1).

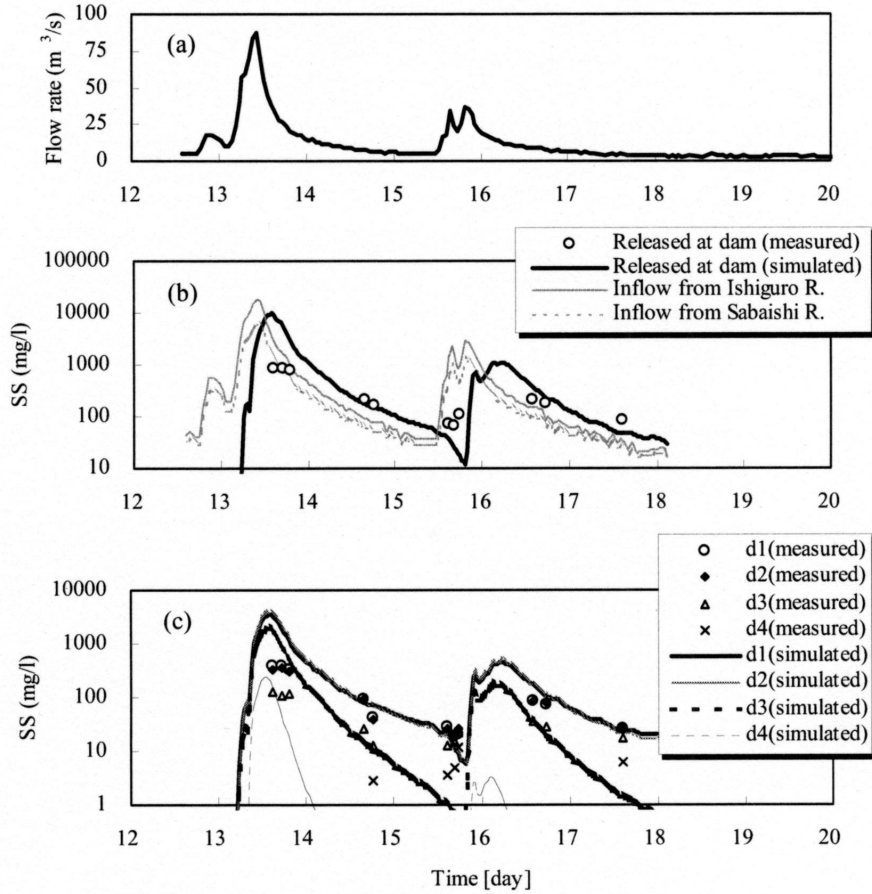
Next, let us consider the phenomena of trapping in a reservoir which is assumed to have a uniform, rectangular channel of length  $L$ , filled from the upstream end at the rate  $Q$  by turbid water containing uniformly distributed sediments with a concentration  $C_j$ . The trapping occurs here only as a result of settling of the SS. If it is assumed that the SS concentration does not change greatly as the water moves over distance  $L$ , all the way through the reservoir, the trapped volume per unit time over distance  $L$ ,  $\Delta V_{sj}$ , is given by the following:

$$\Delta V_{sj} = A_0 w_{sj} \bar{C}_j = A_0 w_{sj} \alpha_j Q^{\beta_j - 1} \quad (7)$$

Here,  $A_0$  is the area of the river bed over length  $L$ .

If the inflow  $Q$  is assumed to change gradually over time while the SS concentration in the channel changes with time while remaining spatially uniform, the trapping efficiency  $\gamma_k$  for flood wave ( $k$ ) is given by Eqs.(1), (7):





Figs. 11 Verification of numerical model: (a) the observed inflow rate; (b) the comparison between the observed and calculated total SS concentrations of released water from the dam; and (c) the comparison between observed and calculated SS concentrations with typical diameters in the released water. (b) also shows the time series for the calculated incoming SS concentrations based on the equation derived from the observed data as shown in Fig.10.

$$\gamma_{jk} = \frac{\int \Delta V_{sj} dt}{\int Q_{sj} dt} = A_0 w_{sj} \frac{\int Q^{\beta_j - 1} dt}{\int Q^{\beta_j} dt} \quad (8)$$

From Eq.(8), it is observed that  $\alpha$  can be removed, and has no effect on  $\gamma$ . In contrast,  $\beta$  appears to have no effect on  $\gamma$  as long as  $Q$  is constant, but once  $Q$  varies with time, as happens during a flood,  $\gamma$  changes in response to  $\beta$ .

The above summary is a simplified model of the phenomenon of sediment trapping in a reservoir, and may be of only approximate application to a general case, but it can be instructive in terms of the relationship between  $\alpha$ ,  $\beta$  and  $\gamma$ .

### 3.5.3 Calculation of trap efficiency

As stated at the beginning of the previous section, the SS simulations were conducted with the reservoir shape, flood condition,  $\alpha$  and  $\beta$  varied. The equations for simply calculating  $\gamma$  were derived from these simulated results. As revealed in 3.5.2, almost no influence from  $\alpha$  is seen on  $\gamma$ , so that simulated results for  $\alpha$  are omitted below.

Hydrological data for ten floods with different peak

discharge were used for the SS simulation. Three values of  $\beta$  were chosen as a reference of the observed values in Table 5. We explain a procedure for deriving a simple expression below, using the Sabaishi River as an example.

Figure12 presents an example of the simulated relationship between  $\gamma$  and  $\beta$  under the same flood and reservoir's topographic conditions. For all the particle size classes,  $\gamma$  decreases monotonically with increase in  $\beta$ . This is because the incoming water discharge changes in an unsteady manner, as shown in Eq.(8).

Figure13(a) and (b) show the simulated relationship between  $\gamma$  and flood index when  $\beta$  is fixed at a value of 2.7. The turnover ratio of a reservoir during a single flood event  $R_f$  is known to be a useful index of  $\gamma$  and flood characteristics<sup>9</sup>, but for this study, the mean residence time  $T_r$ , a parameter which incorporates time, was also examined. Here,  $R_f$  is the total volume of entering water divided by the reservoir water volume just before the flood, and  $T_r$  is the volume of reservoir water just before the flood divided by the mean discharge during the flood period. The results indicate that both  $R_f$  and  $T_r$  have a relatively consistent relation with  $\gamma$ , but  $T_r$  shows a stronger correlation with  $\gamma$ ; it

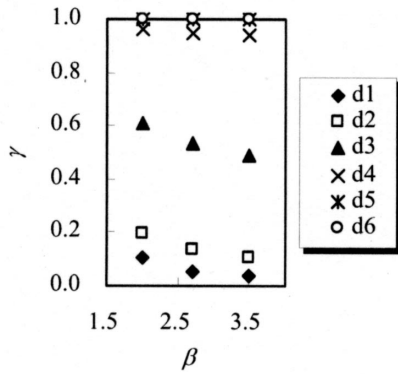


Fig. 12 Relationship between  $\alpha$  and  $\beta$  (fixing flood and topographical conditions)

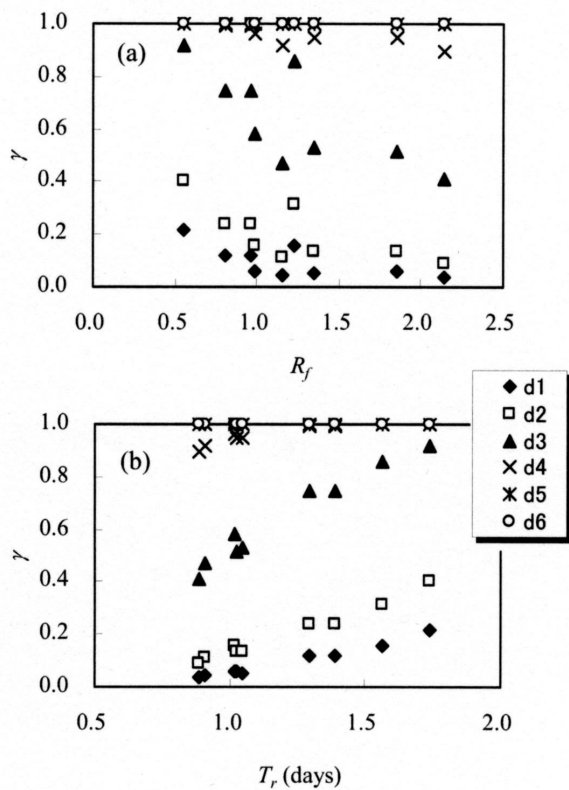


Fig. 13 Relationship between  $\gamma$  and flood indexes ( $\beta=2.7$ )  
( $R_f$ : Turnover ratio per flood event;  
 $T_r$ : mean residence time)

was therefore decided to use  $T_r$  as an index of  $\gamma$  at Sabaishigawa Dam.

Figures 12 and 13 demonstrate the linear relationships of  $\gamma$  with  $\beta$  and  $T_r$ , so it seems likely that  $\gamma$  at typical diameters can be expressed as a linear function of  $\beta$  and  $T_r$ . Therefore, the following expression was conceived as a simple equation for estimating  $\gamma$ , and the coefficients were calculated using the least-squares approximation.

$$\gamma = a \cdot \beta + b \cdot T_r + c \quad (9)$$

Coefficients  $a$ ,  $b$ , and  $c$  can be determined for each particle size class and reservoir shape.

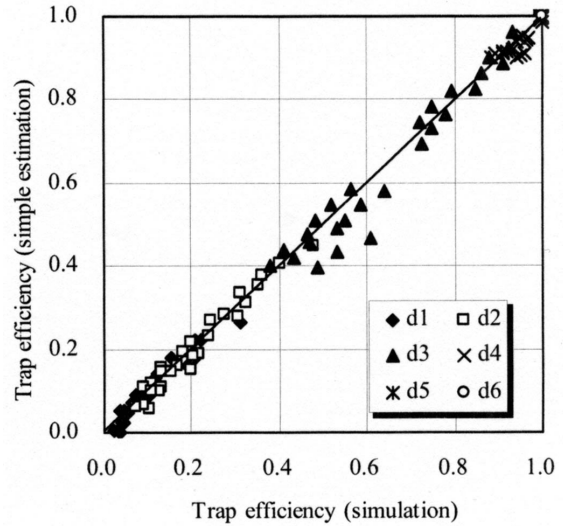


Fig. 14 Comparison of values predicted by simple estimation and numerical simulation

Table 6 Coefficients of equation (9) for simply estimating trap efficiency (example: Sabaishi R.)

Coeff.	Typical particle size class #					
	1	2	3	4	5	6
$a$	-0.058	-0.062	-0.048	-0.007	0.000	0.000
$b$	0.200	0.340	0.580	0.110	0.000	0.000
$c$	0.024	-0.034	0.077	0.850	1.000	1.000

Figure 14 compares the values of  $\gamma$  determined by the simple method outlined above with those determined by the numerical simulations. Table 6 shows the derived coefficients  $a$ ,  $b$  and  $c$  to be used by the simple equation. There was a scatter in a certain particle, but the simple equation accurately reproduced the trap efficiencies derived from the numerical simulation. It should be noted that the above results apply only to the Sabaishi River section.  $a$ ,  $b$  and  $c$  were also calculated for the Ishiguro River section, and showed the same level of the coefficient values as the Sabaishi River section, and the final results for the trap efficiency also had the same level of accuracy as in Fig. 14.

#### 3.5.4 Data selection

In the Sabaishigawa Reservoir, the water level is occasionally lowered during the spring thaw, during which the accumulated sediment is entrained back into the current, resulting in release of the accumulated fine sediment downstream. However, our simulation model is not capable of considering the resuspension of fine sediment by means of "water level lowering operation", so in this study, the years during which the phenomenon was occurred were excluded from the analysis. Accordingly, actual sedimentation data from only 6 calendar years were used.

#### 3.5.5 Parameter identification

Values of  $\alpha$ ,  $\beta$  and  $Q_c$  were determined in order to obtain minimum residues of the following equation:

$$\varepsilon_j = \sum_{i=1}^N | [V_{S0j}]_i - [V_{Sj}]_i | \quad (10)$$

The search ranges of  $\alpha$  and  $\beta$  were selected on the basis of the previous observational reports and the additional survey in the dam. In the present study,  $\alpha$  and  $\beta$  were searched for in the ranges  $1.0 \times 10^{-6} - 8.0 \times 10^{-6}$  and  $1.0 - 4.0$ , respectively, and  $Q_c$  was set to flow rates of  $0 - 20 \text{ m}^3/\text{s}$ .

### 3.5.6 Estimation results

Values of the coefficients identified from Eq.(10) are shown in Table 7. The  $\alpha$  and  $\beta$  values are similar to those of observed SS presented in Table 5, so seem to be appropriate. The measured values reveal the trend of increasing  $\beta$  with decreasing sediment size class; the results in Table 7 show the same trend. There are no published survey-based data on the effects of parti-

cle size on the relationship between SS and flow rate, and it is therefore unknown why  $\beta$  showed the trend described above. Data must be gathered at other dams in the future in order to answer this question. Also, the critical flow  $Q_c$  was lower for fine sediment than for coarse one. Most of the coarse is supplied from river bed, while most of the fine is introduced by erosion of inclines by rainfall and surface flow. The different sources of these sediment types are reflected in different  $Q_c$  values.

Figure 15 compares the estimated and measured volumes of the typical size classes in the Sabaishi River. This does not provide detailed data for annual changes in sedimentation, but on the whole the estimates reproduced the observed data well. The annual trap efficiency for the partially trapped sediment was 20% – 60% (Table 8). This confirms that the influence of the trap efficiency of the fine sediment cannot be neglected when estimating the fine sediment discharge.

Table 7 Identified values of  $\alpha$ ,  $\beta$  for the partially trapped sediment

Class #	Typical size (mm)	Sabaishi R.		Ishiguro R.	
		$\alpha$	$\beta$	$\alpha$	$\beta$
1	0.0035	$6.1 \times 10^{-6}$	3.3	$5.6 \times 10^{-6}$	3.0
2	0.0059	$2.0 \times 10^{-6}$	3.2	$2.5 \times 10^{-6}$	2.9
3	0.015	$3.4 \times 10^{-6}$	2.6	$4.3 \times 10^{-6}$	2.4
4	0.032	$3.0 \times 10^{-6}$	2.4	$6.1 \times 10^{-6}$	2.1
5	0.069	$1.4 \times 10^{-6}$	2.4	$3.6 \times 10^{-6}$	2.2
6	0.16	$2.1 \times 10^{-6}$	1.9	$3.7 \times 10^{-6}$	2.1
Critical discharge		$Q_c=4\text{m}^3/\text{s}$		$Q_c=4\text{m}^3/\text{s}$	

## 4. Summary

In this study, we propose an estimation method of non-uniform sediment discharge using actual results of dam reservoir sedimentation. The method includes developing a calculation technique for trap efficiency of fine sediment and systematizing estimation processes of field surveys and data analysis. The validity of this method is confirmed through the case of the Sabaishigawa Dam, Nigata Prefecture. A flowchart of the proposed procedure is shown in Fig. 1, Chapter 2.

Our estimates of sediment discharge at the Sabaishigawa Dam are reasonably accurate, but this is the only

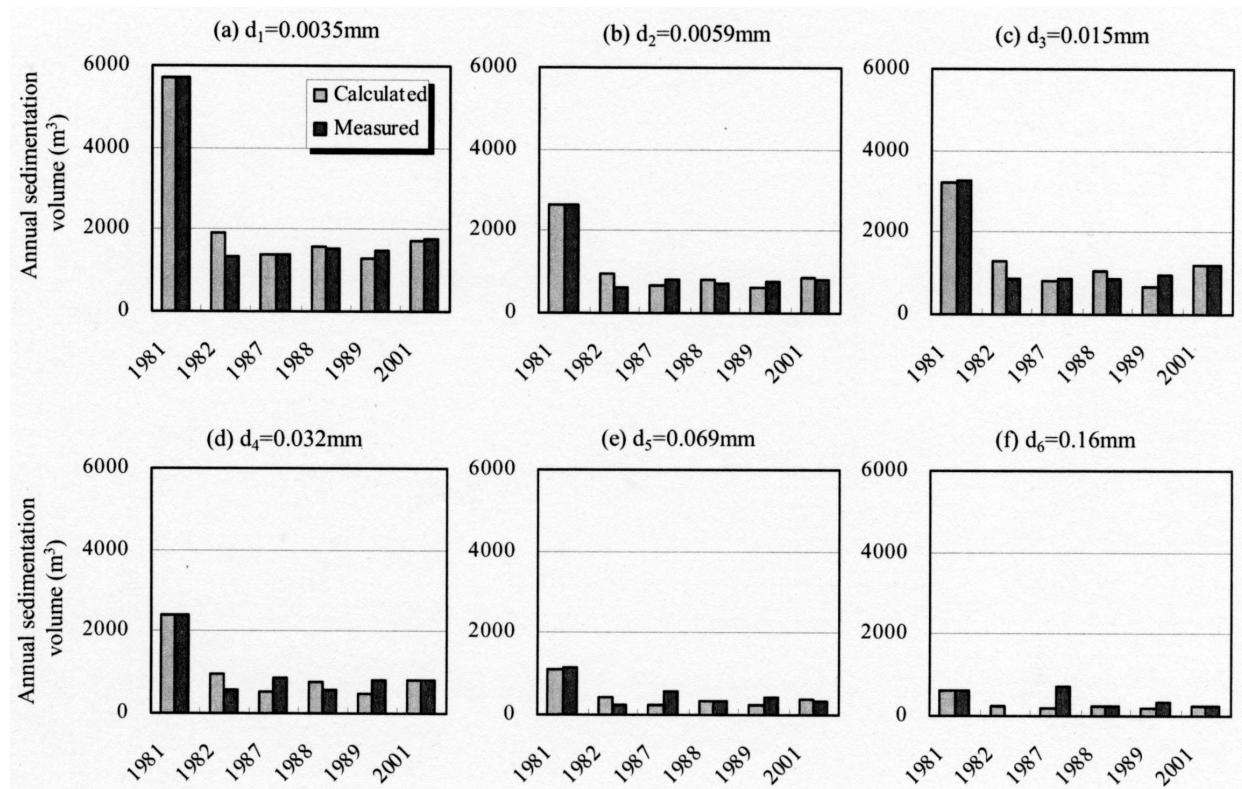


Fig. 15 Estimated results for the partially trapped sediment (ex: Sabaishi R.)

Table 8 Annual trap efficiencies for the partially trapped sediment (estimated results)

	Sabaishi River			Ishiguro River		
	$Q_{sin}$ (m <sup>3</sup> /yr)	$V_s$ (m <sup>3</sup> /yr)	$\gamma$	$Q_{sin}$ (m <sup>3</sup> /yr)	$V_s$ (m <sup>3</sup> /yr)	$\gamma$
1981	5.2x10 <sup>4</sup>	1.6x10 <sup>4</sup>	0.30	7.7x10 <sup>4</sup>	2.8x10 <sup>4</sup>	0.36
1982	2.5x10 <sup>4</sup>	5.8x10 <sup>3</sup>	0.23	3.3x10 <sup>4</sup>	1.1x10 <sup>4</sup>	0.34
1987	8.0x10 <sup>3</sup>	3.8x10 <sup>3</sup>	0.48	1.4x10 <sup>4</sup>	7.8x10 <sup>3</sup>	0.54
1988	1.5x10 <sup>4</sup>	4.7x10 <sup>3</sup>	0.33	2.3x10 <sup>4</sup>	9.7x10 <sup>3</sup>	0.43
1989	6.0x10 <sup>3</sup>	3.5x10 <sup>3</sup>	0.58	1.2x10 <sup>4</sup>	7.4x10 <sup>3</sup>	0.63
2001	1.3x10 <sup>4</sup>	5.3x10 <sup>3</sup>	0.40	2.3x10 <sup>4</sup>	1.1x10 <sup>4</sup>	0.46

Note)  $Q_{sin}$ : Annual sediment inflow volume;  $V_s$ : Annual trapped volume;  $\gamma$ : Annual trap efficiency.

dam to which this method has been applied. The method will be used to model sedimentation at other dams in the future to further verify its applicability.

The modeling procedure described in this study takes into account both coarse and fine sediments, and is a promising method of estimating the loads of a wide range of sediment size classes. The method for obtaining a relationship between the flow rate and the sediment discharge for a dam sedimentation have not been systematized yet, and we hope that this method will prove useful for designing sedimentation measures and general sedimentation management.

#### References:

- 1) K. Ashida, T. Takahashi and M. Michiue: Sediment disaster and its countermeasures in rivers, Morikita Shuppan Co., Ltd, pp.153, 1983. (in Japanese)
- 2) T. Sakurai, J. Kashiwai and M. Oguro: Sedimentation form in dam reservoirs, Civil Engineering Journal, Vol.45, No.3, pp.56-61, 2003. (in Japanese)
- 3) M. Michiue and K. Ashida: Study on hydraulic resistance and bed-road transport rate in alluvial streams, Proceedings of Japan Society of Civil Engineers, No.206, pp.59-69, 1972. (in Japanese)
- 4) K. Ashida, T. Takahashi and M. Michiue: Sediment disaster and its countermeasures in rivers, Morikita Shuppan Co., Ltd, pp.40-42, 1983. (in Japanese)
- 5) J. Kashiwai: Consideration for trap efficiency of fine sediment in dam reservoirs, Engineering for Dams, No.181, pp.21-28, 2001. (in Japanese)